



Calibration and Intercomparison of Filter-Based Measurements of Visible Light Absorption by Aerosols

Tami C. Bond , Theodore L. Anderson & Dave Campbell

To cite this article: Tami C. Bond , Theodore L. Anderson & Dave Campbell (1999) Calibration and Intercomparison of Filter-Based Measurements of Visible Light Absorption by Aerosols, Aerosol Science & Technology, 30:6, 582-600, DOI: [10.1080/0278682993044435](https://doi.org/10.1080/0278682993044435)

To link to this article: <https://doi.org/10.1080/0278682993044435>



Published online: 30 Nov 2010.



Submit your article to this journal [↗](#)



Article views: 1748



Citing articles: 473 View citing articles [↗](#)



Calibration and Intercomparison of Filter-Based Measurements of Visible Light Absorption by Aerosols

Tami C. Bond, Theodore L. Anderson, and Dave Campbell

DEPARTMENTS OF ATMOSPHERIC SCIENCES, CIVIL AND MECHANICAL ENGINEERING,
UNIVERSITY OF WASHINGTON, SEATTLE, WA (T.C.B.), JOINT INSTITUTE FOR THE STUDY
OF THE ATMOSPHERE AND OCEAN, UNIVERSITY OF WASHINGTON, SEATTLE, WA
(T.L.A.), CROCKER NUCLEAR LABORATORY, UNIVERSITY OF CALIFORNIA AT DAVIS,
DAVIS, CA (D.C.)

ABSTRACT. Data on light absorption by atmospheric particles are scarce relative to the need for global characterization. Most of the existing data come from methods that measure the change in light transmission through a filter on which particles are collected. We present a calibration of a recently developed filter-based instrument for continuous measurement of light absorption (model PSAP, Radiance Research, Seattle, WA) that has been incorporated in several measurement programs. This calibration uses a reference absorption determined as the difference between light extinction and light scattering by unaltered (suspended) particles. In addition, we perform the same calibration for two other common filter-based methods: an Integrating Plate and the Hybrid Integrating Plate System. For each method, we assess the responses to both particulate light scattering and particulate light absorption. We find that each of the instruments exhibits a significant response to nonabsorbing aerosols and overestimates absorption at 550 nm by suspended particles by about 20–30%. We also present correction factors for the use of the PSAP.

INTRODUCTION AND BACKGROUND

The quantity of interest for assessing the effect of light-absorbing particles on global and regional climate is the *absorption coefficient*, σ_{ap} , which has dimensions of inverse distance. The subscript *ap* refers to the absorption by particles (excluding extinction by scattering or by gaseous components). Measurements of σ_{ap} are relatively scarce (Heintzenberg et al. 1997). Most of the existing data are from filter-based methods, which derive absorption from the change in light transmission through a filter on which particles have been collected. These

methods include the Integrating Plate (IP; Lin et al. 1973), the Hybrid Integrating Plate System (HIPS; a variant of the system discussed by Campbell et al. 1995), the Particle Soot Absorption Photometer (PSAP; Radiance Research, Seattle, WA), and the Aethalometer (Hansen et al. 1982). The PSAP and the Aethalometer produce real-time measurements. Other methods of measuring σ_{ap} include the photoacoustic method (Adams 1989; Arnott et al. 1997; Moosmüller et al. 1998) and the integrating sphere (IS; Fischer 1970; Heintzenberg 1982). This paper focuses on an intercomparison of the IP, the HIPS, and

the PSAP. A description of the PSAP, which has not previously appeared in the literature, is given in the following section.

Each of the methods discussed above has been used in field measurements of σ_{ap} . Waggoner et al. (1981) present IP data taken in urban and rural areas in the United States. Clarke (1989) reports 6 years of data collection in remote environments using the integrating sandwich, a variant of the IP. The Interagency Monitoring of Protected Visual Environments (IMPROVE) program has produced a large data set of measurements from the U.S. National Parks using HIPS (Malm et al. 1994, 1996). The PSAP is used in ground-based monitoring by the National Oceanic and Atmospheric Administration's Climate Monitoring and Diagnostics Laboratory (NOAA-CMDL) and in field campaigns such as the Aerosol Characterization Experiment (ACE-1, ACE-2) of the International Global Atmospheric Chemistry (IGAC) program (e.g., Quinn et al. 1998).

These applications of filter-based methods have been undertaken without the benefit of a calibration that uses an independent measurement of σ_{ap} . Lin et al. (1973) validated the IP measurement within a factor of 2 by loading filters with laboratory aerosols of "known optical properties." The HIPS was calibrated with reflectance and transmittance standards traceable to NIST (Campbell et al. 1995). A calibration of the PSAP has not appeared in the literature. Another technique that has been used as a measure of absorption, the IS (Fischer 1970), is actually calibrated as a measure of Monarch-71 soot mass (Heintzenberg 1982). Despite the fact that it was never compared with an absolute measurement of light absorption by suspended particles, the IP with Nuclepore filters has frequently been taken as a reference measurement of σ_{ap} (Bodhaine et al. 1992; Bodhaine 1995; Clarke 1982b; Clarke 1989; Waggoner et al. 1981; Edwards et al. 1983; Heintzenberg and Leck 1994). Clarke (1982a) recognized the need for corrections to the method, attributing errors to internal reflections by the filter. He developed a correction

scheme based on modeling and tests with different configurations of the IP (but no absolute standard). The first calibration of the IP as a measure of σ_{ap} to appear in the refereed literature (Horvath 1997) found that the IP significantly overestimates σ_{ap} , especially under conditions of high particulate light scattering. Horvath (1997) used the difference between extinction and scattering as the reference measurement of light absorption. In this paper, we present a similar calibration of the PSAP.

Intercomparisons of light absorption measurement methods have been reported. Sadler et al. (1981) compared the responses of the IP and a laser transmission method and found that the IP measured lower by about a factor of 3. The First International Workshop on Light Absorption by Aerosol Particles, held in 1980 in Fort Collins, CO (Gerber and Hindmann 1982) provided an opportunity for participants to measure a common aerosol. Bennett and Patty (1982) compared the IP with a photoacoustic detector and found that the IP exhibited a greater response to nonabsorbing aerosol. Clarke et al. (1987) compared the IP with the integrating sphere. In this work, we compare the PSAP to two other filter-based measurements: the IP and the HIPS.

EMPIRICAL MODEL

As will be discussed, several factors can lead to overestimation of absorption by filter-based measurement methods. The focus of this paper is on providing empirical observations to aid in interpreting filter-based measurements rather than offering a theoretical assessment of these factors.

We use a simple empirical model to represent the instrumental response, i.e., the apparent absorption by an aerosol deposited on the filter. We assume that the instrumental response is a linear function of both the absorption coefficient, σ_{ap} , and the scattering coefficient, σ_{sp} , such that

$$\sigma_{meas} = K_1\sigma_{sp} + K_2\sigma_{ap}. \quad (1)$$

For an ideal measurement of absorption, K_1 would equal 0 and K_2 would equal unity. This

model is similar to the method of Horvath (1997), who suggested corrections based on the ratio between absorption and scattering or extinction measurements. This simple model ignores some nonlinear effects that are discussed in the following sections. Another correction proposed by Petzold et al. (1997), based on the fraction of light-absorbing mass in the sample, cannot be applied to a purely nonabsorbing sample.

Response to Scattering

Filter-based methods will report an artifact absorption if transmission through the loaded filter is reduced by particulate light scattering. Each of the filter-based methods incorporates features designed to minimize the response to light scattering. The IP uses an opal glass diffuser to transmit forward-scattered light and relies on index of refraction matching between the particle and the polycarbonate Nuclepore surface to minimize the sensitivity to backscattered light (Lin et al. 1973). The HIPS and PSAP rely on the optically diffusive properties of the filter medium itself to minimize the sensitivity to forward scattering. To reduce the sensitivity to backscattering, the HIPS measures and accounts for the change in backscattered light, while the PSAP uses fiber filters which allow the particles to become partly or completely embedded in an optically diffusive environment.

Despite these design features, some sensitivity to light scattering by particles could exist for each of the methods. Other researchers (Bennett and Patty 1982; Ruoss et al. 1992; Petzold et al. 1997) have reported that filter-based measurements of absorption respond to nonabsorbing particles. We determine this sensitivity by including the particulate light scattering as an independent variable in a multiple linear regression; however, the sensitivity can also be determined by simply measuring the response of a method to a nonabsorbing (white) salt such as ammonium sulfate or sodium chloride.

The response of a filter-based measurement to scattering aerosol depends on at least three

factors that are not accounted for by using a constant value of K_1 : (1) *Presence of scattering particles on the filter*. The PSAP shows a decreased response to scattering when the filter is loaded with nonabsorbing particles. The quantity of white particles required to change this response by 10% is quite large, probably greater than would be obtained in a typical field measurement. (2) *Presence of absorbing particles on the filter*. The response to white particles increases when absorbing particles are present on the filter, presumably because white particles can scatter light toward the dark particles, providing more opportunities for the dark particles to absorb light. This effect will be discussed in more detail later. (3) *Size distribution of the particles*. The backscattering by particles depends on their size.

The linear correction scheme does not capture the variation in the response to scattering discussed above. Our approach does constitute, however, a significant, first-order correction that can readily be applied to absorption measurements whenever simultaneous light scattering data are available.

Response to Absorption

The instrumental response to absorption is enhanced over the value of absorption in the atmosphere if the particles have multiple opportunities to absorb light. To the extent that the particles are embedded in the filter medium, scattering of light by the filter allows the same photon to pass through the layer of absorbing particles more than once so that there are multiple opportunities for absorption. A correction factor is usually applied to a filter-based measurement to estimate absorption by suspended particles.

When scattering particles are deposited on a filter, multiple opportunities for absorption can result even if the particles are not embedded in the filter (e.g., Bennett and Patty 1982). This effect can cause a variation in the response to absorption, which, again, is not represented by the use of the linear correction factor K_2 .

PSAP

Operation

The PSAP produces a continuous measurement of absorption by monitoring the change in transmittance across a filter using a 567 nm LED. (The calibration described here is referenced to 550 nm for consistency with the central wavelength of the TSI nephelometer.) A sketch of the operating portion of the instrument is given in Figure 1. The simplest calculation of absorption coefficient, in units of m^{-1} , is given by the equation below for any filter-based method:

$$\sigma'_{\text{ap}} = \frac{A}{V} \ln \left[\frac{I_0}{I} \right], \quad (2)$$

where A is the area of the sample spot (the PSAP assumes an area of $1.783 \times 10^{-5} \text{ m}^2$; however, the actual spot area is somewhat larger and varies from unit to unit, as described by Equation (6)), V is the volume of air drawn through the filter during a given time period in m^3 , and I_0 and I are the average filter transmittances during the prior time period and the current time period, respectively.

Equation (2) does not account for the magnification of absorption by the filter medium or for nonlinearities in the response of the unit as

the filter is loaded. The value actually reported by the PSAP (σ_{PSAP}) includes an empirical calibration that accounts for both of these effects:

$$\sigma_{\text{PSAP}} = \frac{\sigma'_{\text{ap}}}{2(0.5398\tau + 0.355)}, \quad (3)$$

where τ is the filter transmission ($\tau = 1$ for an unloaded filter; this value is reset by the user after installation of each new filter). The empirical calibration was determined by the manufacturer using a procedure similar to the one described in this paper: a comparison between the instrument response and the difference between extinction and scattering. The more extensive calibration tests presented herein are a correction to the manufacturer's calibration. During our tests, we investigated the dependence of the calibration on filter transmission and found that the manufacturer's equation accounted for this effect satisfactorily. The calibrations presented here are valid as long as the filter transmission is greater than 0.7. For individual instruments, inaccurate assumptions about flow rate and spot size can result in significant errors in measured values of absorption. The reported absorption coefficient can be corrected for these effects by using

$$\sigma_{\text{adj}} = \sigma_{\text{PSAP}} F_{\text{flow}} F_{\text{spot}}, \quad (4)$$

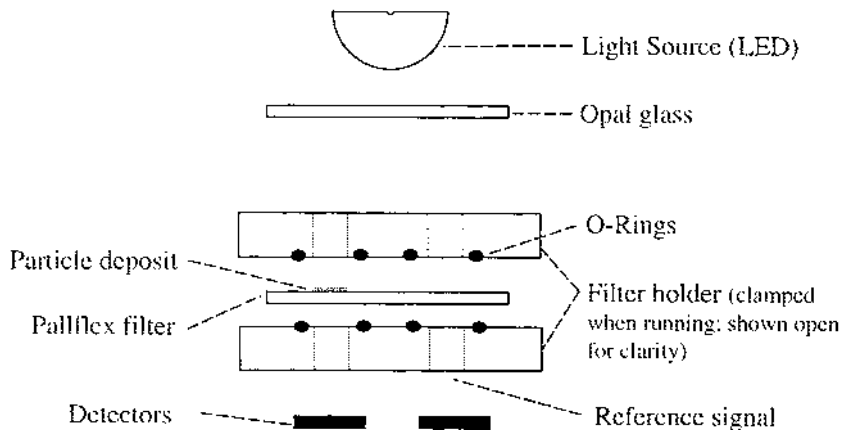


FIGURE 1. Cross-section of the filter setup in the PSAP. The sample is drawn through one of the holes, shown on the left, and the particles are deposited on the filter. Filtered air is drawn through the hole shown on the right for a reference measurement.

where the subscripts *adj* and PSAP stand for the values that have been adjusted and that are stated by the instrument, respectively; $F_{f\ low}$ is a flow correction factor; and F_{spot} is a spot-size correction factor. Their determination requires that the user measure the actual flow rate and spot size, as discussed below.

We have found that the sample flow rate measured internally by the PSAP can be in error by as much as 20%. Users of the instrument should measure the flow rate directly and derive the flow correction factor, $F_{f\ low}$, as follows:

$$F_{f\ low} = \frac{\sigma_{calib}}{\sigma_{PSAP}} = \frac{Q_{PSAP}}{Q_{meas}}, \quad (5)$$

where Q_{PSAP} is the air flow rate stated by the PSAP and Q_{meas} is measured with a high-accuracy flow meter, such as an electronic bubble flow meter (adjusted, if necessary, to the desired temperature and pressure). This procedure amounts to a recalibration of the instrument's internal mass flow meter.

If the seal between the holder and the filter is imperfect, the spot area may be altered. An imperfect seal can be caused by O-rings that are too large or by a warped filter holder. For example, the absorption measured by one of our instruments with a slightly warped filter holder was found to be about 30% low. Users can determine the existence of a good seal by close examination of the spot made by an absorbing aerosol. If the spot has clean, sharp edges, the seal is most likely adequate. If the edges appear fuzzy, the absorption measurement is questionable and the user should either obtain a new filter holder or replace the O-rings with a different style.

We observed some variation in spot size among instruments due to minor changes in design or differences in machining of the filter holder. To account for these differences, a careful measurement of the spot diameter can be used in the following equation:

$$F_{spot} = \frac{\sigma_{calib}}{\sigma_{PSAP}} = \left(\frac{D_{meas}}{D_{calib}} \right)^2, \quad (6)$$

where $D_{calib} = 5.1$ mm is the spot diameter of

the reference PSAP calibrated by the manufacturer and D_{meas} is the diameter measured for the individual instrument.

Instrument Precision

Because routine calibration of the PSAP is not possible, the user relies on the manufacturer's calibration and the consistent performance of the instrument. In this section, we discuss noise and unit-to-unit variability using field measurements made in the spring of 1997 at a coastal station (Cheeka Peak, WA) that samples both marine and moderately polluted continental air. Details of the experimental setup can be found in Anderson et al. (1998). The analysis is based on measurements of the sub- μ m particles (particles with low RH aerodynamic diameters below 1 μ m); results for sub-10 μ m particles were not significantly different.

After the corrections for flow rate and spot size, linear regressions of the field data revealed that two of the three PSAPs agreed within 1% of each other, while the third differed by 4% from the other two. Based on this result, we estimate that unit-to-unit variability is within $\pm 6\%$ of 95% confidence, or

$$\epsilon_{slope}(\text{Mm}^{-1}) = 0.06\sigma_{ap, meas}. \quad (7)$$

The ability to measure low values is limited by instrument noise, which has been estimated by Anderson et al. (1998) from PSAP readings during the measurement of particle-free air. A 95% confidence interval for instrument noise is

$$\epsilon_{noise}(\text{Mm}^{-1}) = 0.18\sqrt{\tau_0/\tau}, \quad (8)$$

where τ is the averaging time and $\tau_0 = 24$ min.

To estimate uncertainties due to changes in face velocity, we compared field measurements of instruments operating at 1 lpm and 2 lpm. We found no differences exceeding the 6% instrumental precision discussed above.

Unit-to-unit variability at higher levels of absorption is also of interest. Figure 2 shows the percentage difference between two units as a function of absorption level during the calibration tests. The instruments generally agreed to better than 5%; notable exceptions are sev-

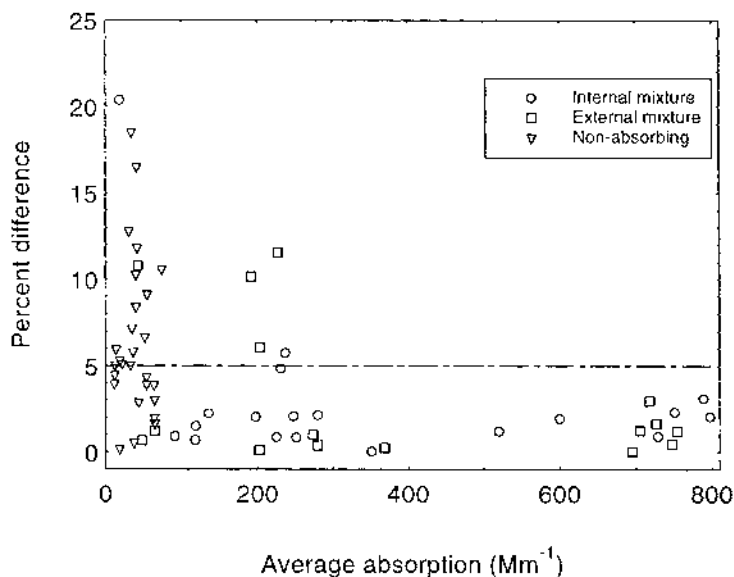


FIGURE 2. Percent difference between PSAPs for calibration tests.

eral tests with nonabsorbing aerosol, where the PSAPs measured an artifact absorption, and a few tests with externally mixed aerosol.

IP AND HIPS

The IP arrangement was that recommended by Clarke et al. (1987) with the particle-laden surface of the filter positioned away from the opal glass and toward the detector. We used Nuclepore filters with a pore diameter of $0.6 \mu\text{m}$. For the particle sizes and face velocities used in this experiment, these filters have a collection efficiency of 80–90% (Liu and Lee 1976).

We measured absorption at 4 wavelengths: 435, 525, 660, and 800 nm. The IP response we present in this work is the inferred response at 550 nm, interpolated using the power-law wavelength dependence between 525 and 660 nm. The wavelength dependence of absorption, as determined from the IP measurements, was approximately proportional to $\lambda^{-0.3}$. Analysis of a nigrosin solution at UC Davis showed that the refractive index was constant with wavelength. A wavelength dependence of $\lambda^{-1.0}$ is

expected for particles that are “small compared to the wavelength of light” (van de Hulst 1957), but the accumulation-mode particle sizes used in this study do not meet that criterion. Mie calculations for particles with refractive index $1.67 + 0.26i$ show that the expected relationship is $\lambda^{-0.5}$ for 400-nm particles.

The HIPS was a variant of the system described by Campbell et al. (1995). The samples were analyzed according to the methodology currently used for IMPROVE sampling. In this method, the reflectance (R) of a filter is measured by placing the filter at one end of an integrating sphere. Transmittance (T) is measured simultaneously with an integrating plate, and the absorption coefficient is calculated as

$$\sigma'_{\text{ap}} = \frac{A}{V} \ln \left[\frac{1-R}{T} \right]. \quad (9)$$

Because of the large number of filters analyzed by this system, the filters are held in a photographic slide changer; there is a gap between the filter and the integrating sphere or plate that results in some loss of light. An empirical correction factor is applied to account for this effect,

both in analysis for the IMPROVE network and for the data presented here.

The HIPS operates at a wavelength of 633 nm, and we did not make any adjustments to account for the wavelength difference. Based on the wavelength dependence given by the IP, the HIPS results should be 5% lower than the other measurements; that is, the absorption calibrations given later should be multiplied by 0.96.

CALIBRATION METHOD

Highly concentrated aerosols were generated in the laboratory at the University of Washington and simultaneous measurements of light absorption by these aerosols were made with several instruments. While the concentration of particles in the aerosol was much higher than in atmospheric aerosols, the test durations were much shorter than those typical of ambient tests. The total mass loading on the filters was similar to that common in ambient tests.

The tests took place in the laboratory at the University of Washington during November of 1996 and January, February, June, and August of 1997. Each instrument was present for different subsets of the experiment. An overview of the intercomparison measurements is given in Table 1, and the experimental setup for one set of tests appears in Figure 3.

The measurements we will compare were made simultaneously, and careful attention was

given to aligning the beginning and ending times for each instrument. For instruments that measure in real-time—the OEC, nephelometer, and PSAP—the measured value of absorption is the average over the time between the beginning and ending time of the test. The beginning and ending times also governed the routing of the particle-laden flows through the filters for methods that intrinsically measure a test average—the IP and HIPS. Tests were generally either 2 or 5 min long.

Reference Absorption

Our “reference” absorption is the difference between extinction and scattering; our extinction measurements are matched to the scattering measurements for white particles. Absorption measured by this method should closely approximate light absorption in the atmosphere. Opportunities for multiple absorption of scattered light are limited because the particles are not highly concentrated, and artifacts caused by the presence of the filter medium are nonexistent. When a “known” aerosol is used as a reference, assumptions of a refractive index and size distribution are critical, whereas our reference method does not require knowledge of these parameters.

The disadvantage of this method is the determination of absorption as the small difference of two large numbers. Figure 4 shows scatter-

TABLE 1. Overview of instruments participating in intercomparison.

Instrument	Filter Type	Wavelength (nm)	Meas. Period	No. Tests
Optical Extinction Cell (OEC)	—	550 nm	Nov 96	125
Radiance Research		(adj)	Jan, Feb, Aug 97	
Nephelometers (2)	—	450, 550,	Nov 96	125
TSI, Inc.		700 nm	Jan, Feb, Aug 97	
Particle Soot Absorption Photometer (PSAP)	Pallflex	550 nm	Nov 96	63
Radiance Research, Seattle, WA	E70-2075W		Jan, Feb, Aug 97	
Integrating Plate (IP, 4 wavelengths)	Nuclepore	435, 525,	Jan 97	24
University of Washington	0.6 μ m	600, 800 nm		
Hybrid Integrating Plate System (HIPS)	Teflo	633 nm	Jan 97	25
Operated by UC Davis Personnel				

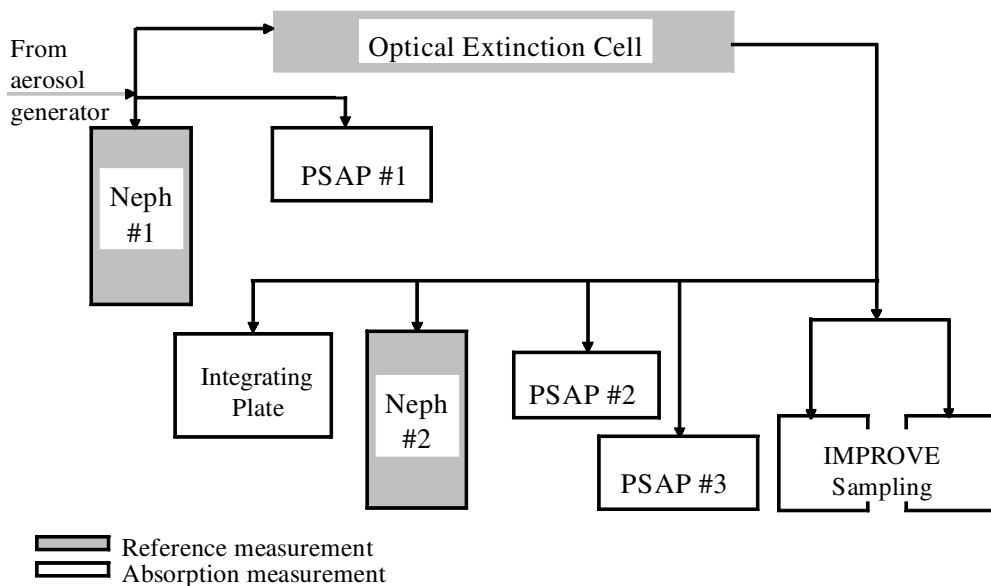


FIGURE 3. Typical experimental setup. At times, the instruments marked “IMPROVE Sampling” and “Integrating Plate” were not present.

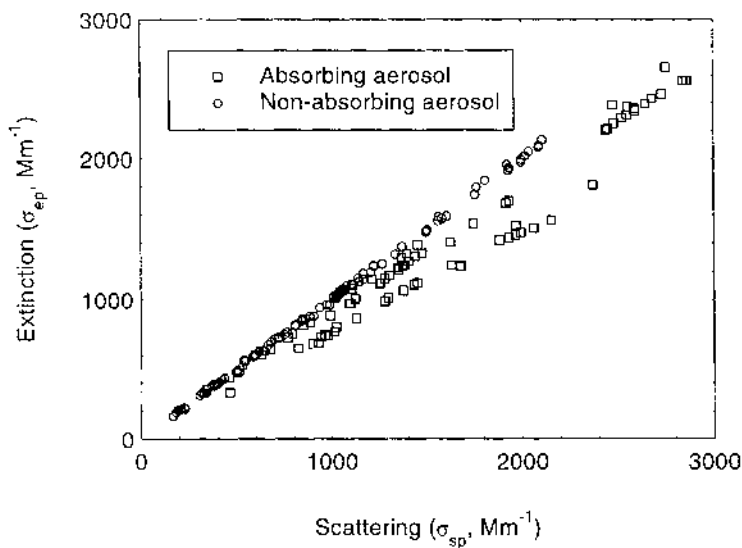


FIGURE 4. Extinction versus scattering for all calibration tests.

ing versus extinction for the 169 tests used in this calibration. Because of the forced match between the extinction and scattering for white

aerosol tests (discussed below), these tests lie along the 1:1 line with the small deviations reflecting the measurement error. For absorbing

aerosols, the deviation from the 1:1 line indicates the size of the effect we are trying to quantify. Even a small uncertainty in either extinction or scattering may result in a large error in the reference absorption.

Scattering by particles is measured by two 3-wavelength nephelometers (TSI, Inc., Model 3563). This instrument has been extensively characterized (Anderson et al. 1996), and we followed the calibration and measurement protocols and adjustments for angular nonidealities recommended by Anderson and Ogren (1998). Following these procedures, the precision uncertainty in this measurement was shown to be within 1%, while the accuracy was within 7%.

We determined the extinction at a single wavelength of approximately 550 nm with a single-pass optical extinction cell (OEC, Radiance Research). In this instrument, the broadband light from the source passes through an opal glass diffuser, travels down the measurement volume (which is 6.37 m long), and is collected by a lens. The lens, designed to eliminate the contribution of forward-scattered light by limiting the viewing angle, focuses the light on an aperture, directly behind which is a solid-state detector (GaAs). The output of the instrument is proportional to the transmitted light intensity divided by the light intensity at a reference detector located near the source, thus accounting for shifts in light intensity of the source. Bandpass filters with 70 nm bandwidth are located immediately in front of both detectors, which are actively temperature controlled at about 40°C. The output at zero-extinction (I_0) is measured as filtered air is passed through the device. Light extinction by particles is calculated by measuring the output of the OEC as the sample air is passed through it (I) and applying the equation

$$b_{\text{ep}} = \ln(I_0/I)/L, \quad (10)$$

where L is the length of the OEC. For these tests, a typical value of I_0/I is 1.01, or a 1% change in light extinction due to the aerosol.

The sensing volume of the OEC is a closed tube through which the sample flow of approx-

imately 100 L/min is drawn. The walls of the sample volume are covered with a rough black foam, which absorbs the light that is scattered out of the sample volume.

The OEC manifests a significant response to changes in air flow through the sample volume, resulting in an apparent drift if the air flow through the device is changed. We maintained a constant air flow rate at all times, and we allowed the OEC to stabilize at a constant air flow rate for a minimum of 2 h (often overnight) before beginning any tests. We also measured the zero-extinction output (I_0) before and after each test and used the average of the two in Equation (10). This adjustment was not systematic and its absolute magnitude affected the extinction coefficient by an average of 0.6%. Ninety-five percent of the drift adjustments were below 2% of the extinction coefficient, meaning that the change in the measurement of transmitted light was lower than 0.01%.

To assess the possibility of particle losses in the OEC, we installed one nephelometer upstream of the OEC and one downstream. The nephelometer measurements compared well. The average ratio between the larger and smaller measurement in each pair is 1.01 and 95% of the measurements are within 2% of each other.

Measurements of extinction and scattering at the same wavelength of light should be identical for nonabsorbing aerosol. However, the wavelengths of the two instruments are not precisely matched, and the scattering efficiency of small particles is strongly dependent on wavelength. To account for this effect, we determined an adjustment that would force a match between the OEC and the nephelometer. This adjustment, based on 82 measurements of nonabsorbing aerosol (ammonium sulfate and sodium chloride), is

$$\sigma_{\text{ep,true}} = \sigma_{\text{ep,meas}} \times (1.050 \pm 0.006). \quad (11)$$

The uncertainty is the 95% confidence interval from a linear regression. The adjustment remained quite constant over time. This adjustment means that the following are true.

1. Our reference absorption measurement is ultimately referenced to the accuracy of the nephelometer;
2. we assume that our laboratory salts are truly nonabsorbing; and
3. we assume that the nephelometer-based adjustment to the OEC applies identically to extinction due to absorption and due to scattering.

Table 2 summarizes the sources of uncertainty in the reference measurement. The uncertainties of 4.1% in the OEC and 1% in the nephelometer contribute to the uncertainty in the difference. The 7% uncertainty in the accuracy of the nephelometer is applied after the difference is taken. Assumption (3) introduces an uncertainty if the OEC adjustment is required because of a wavelength difference between the nephelometer and the OEC and if the wavelength dependence of the scattering differs from that of the absorption. We estimate this uncertainty, based on our measurements, as 4% of the reference absorption to 95% confidence. The uncertainty varies with the relative magnitudes of the scattering and extinction. When scattering contributes 75%, 90%, or 95% of the extinction, the uncertainty is 18%, 42%, or 84% of the difference, respectively. These random uncertainties are applicable to individual measurements of the reference absorption. The uncertainty of

the calibration is lower than that for individual measurements because we have included several measurements over a wide range and statistically analyzed the relationship between the measured and reference absorption.

The large uncertainties for weakly absorbing aerosol highlight the potential uncertainties inherent in using the difference between extinction and scattering to determine a reference absorption. However, any reference method involves uncertainties, whether they result from extinction cell characteristics, interactions with the filter medium, a refractive index assumption for "known" aerosols, or the stability of the "resonator quality factor" for the photoacoustic method. We suggest that this reference for light absorption is most closely representative of atmospheric absorption at visible wavelengths and that the measurement community would benefit from further calibration measurements using this technique with an improved (stabilized and better characterized) extinction cell.

Aerosol Generation

For a light-absorbing material, we used the water-soluble form of nigrosin (Aldrich #19, 828-5). A common black pigment, nigrosin is a short-chain polyaniline consisting of 8 nitrogen-linked aromatic carbon rings. The chemical formula is $C_{48}N_9H_{51}$. Its absorption spectrum is

TABLE 2. Sources of error in reference measurement.

Description	Estimation Method	ϵ (95%)
OEC		
Repeatability	Comparison with nephelometer	3.2%
Zero drift	Zero comparison before and after test	2.0%
Losses	Nephelometer comparison upstream/downstream	1.4%
λ adjustment	Comparison with nephelometer	0.6%
Total		4.1%
Nephelometer		
Repeatability	Anderson and Ogren, 1998	1.0%
OEC minus Neph		
Neph accuracy	Anderson et al. 1996	7%
λ adjustment	Theoretical, using observed λ dependence of scattering and absorption	4%

extremely broad and flat over the entire visible range (Justus et al. 1993). In a previous aerosol study (Garvey and Pinnick 1983), the refractive index of pure nigrosin was taken to be 1.67–0.26*i*.

Water solutions of pure nigrosin, pure ammonium sulfate, and various mixtures of the two were nebulized using bubblers, as shown in Figure 5. The resulting droplets were dried and then passed through a 1- μ m impactor (aerodynamic diameter) to generate submicrometer aerosol particles. The fraction of extinction due to scattering ($\sigma_{sp}/(\sigma_{ap} + \sigma_{sp})$), known as the single-scatter albedo (ω_0), is a measure of the “whiteness” of the aerosol; for a pure white aerosol, $\omega_0 = 1.0$. We used aerosols with single-scatter

albedos ranging from 0.50 to 1.0, as shown in Table 3.

Morphologies for each particle type were examined by transmission electron microscopy and in all cases found to be spheroidal and internally uniform (no evidence of separate crystalline phases within particles). Observed particle sizes were from 0.1 to 0.5 μ m in diameter, which is similar to accumulation mode atmospheric particles.

The mass absorption efficiency of nigrosin particles has not been measured previously. For six of our tests, aerosol mass was determined by the weighing of nuclepore filters and nigrosin mass could be estimated using the approximate mass fractions given in Table 3. These tests indi-

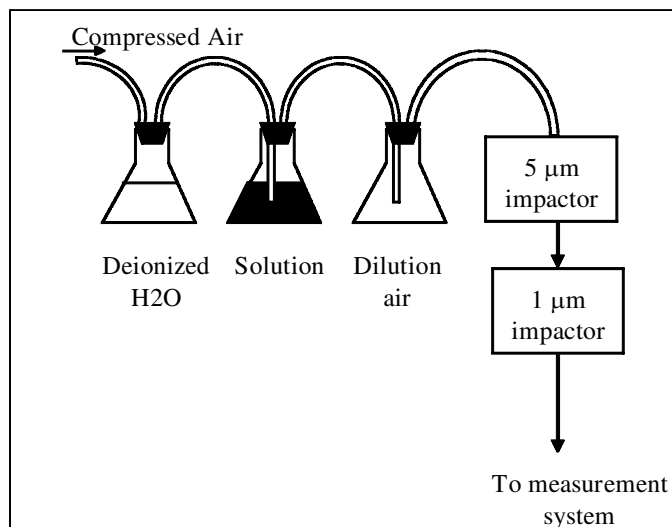


FIGURE 5. Aerosol generation system.

TABLE 3. Solutes used in aerosol generation system. The solvent was distilled, deionized water in all cases. A small amount of isopropanol was added to solutions containing nigrosin to prevent foaming.

Aerosol code	Composition ^a	Average b_{ep} (Mm^{-1})	Approx. single-scatter albedo
amsu	(NH ₄) ₂ SO ₄	1060	1.00
NaCl	NaCl	1580	1.00
an76	4:1 nigrosin to (NH ₄) ₂ SO ₄	1520	0.76
an90	10:1 nigrosin to (NH ₄) ₂ SO ₄	1530	0.90
an95	20:1 nigrosin to (NH ₄) ₂ SO ₄	2590	0.95
nigr	Nigrosin	590	0.5

^a Specified ratios are given in terms of mass and are approximate ($\pm 10\%$).

cated a mass absorption efficiency of $3 \text{ m}^2 \text{ g}^{-1}$, uncertain to about a factor of 2. Thus, nigrosin is similar to elemental carbon (EC) in its relatively high absorption efficiency. Estimates of the absorption efficiency of EC are about $10 \text{ m}^2 \text{ g}^{-1}$ based on Mie theory (Bergstrom 1973) and about $6 \text{ m}^2 \text{ g}^{-1}$ based on measurements of fresh smoke (Dobbins et al. 1994).

The concentration of particles generated by this method is not entirely repeatable and the concentrations drift over a period of minutes. However, the comparison tests were fairly short (30 s to 5 min) and the readings were simultaneous. Thus, any variations in the characteristics of the aerosol should not affect the comparison between instruments.

RESULTS AND DISCUSSION

Statistical Analysis

Values of K_1 and K_2 , representing the response of the instrument to scattering and absorption, respectively, are given in Table 4. Although a multiple linear regression is the simplest method of determining these values, this approach is questionable because there is error in the "independent" variables (the measured values of scattering and absorption) and because the uncertainties are different for each data point. We determined the coefficients K_1 and K_2 with a weighted-least-squares method, following the method of York (1966). In this approach, the quantity minimized is the sum of the squares of

the perpendicular distance to the line, with each point weighted by the inverse of its squared uncertainty.

The uncertainties given in Table 4 bound a 95% confidence interval and include the standard error from the regression as well as the uncertainties in the accuracy of the reference measurement (given under "OEC - Neph" in Table 2).

Our reference absorption is evaluated at 550 nm, and applying the calibration factors given in the table results in an estimate of absorption at that wavelength. The actual wavelength sensed by the absorption instruments differs from 550 nm, and this introduces a further uncertainty which is also included in the 95% confidence limits in the table. To illustrate, the light source of the PSAP operates at 567 nm, so the value of K_2 implicitly includes a wavelength adjustment and should be slightly altered if the spectral dependence of the aerosol being measured differs from that of the calibration aerosol. Assuming that the wavelength dependence of atmospheric aerosol may be as high as λ^{-1} , this consideration introduces an additional uncertainty of 2% into the value of K_2 .

PSAP response to scattering aerosol

The derived value of K_1 for the PSAP is 0.02 ± 0.02 , meaning that about 2% of the light scattered is interpreted as absorption and that the apparent single-scatter albedo of pure white aerosol is 0.98. The 95% uncertainty range in-

TABLE 4. Response of instruments to scattering and absorption. The number of tests for each comparison and the r^2 for each analysis are included. The uncertainties bound a 95% confidence interval and include the standard error from the least-squares analysis, as well as possible systematic uncertainties in the reference absorption.

Instrument	K_1^*	K_2^{**}	N	r^2
PSAP	0.02 ± 0.02	1.22 ± 0.11	63	0.94
IP, adjusted to 550 nm	0.09 ± 0.03	1.23 ± 0.13	24	0.91
HIPS	0.04 ± 0.04	1.33 ± 0.26	25	0.82

*Values of $K_1 > 0$ indicate a response to scattering. For ease of use, these values have been determined using nephelometer data that are not corrected for angular nonidealities.

**Values of $K_2 > 1$ indicate an exaggeration of absorption even after correction for the response to scattering.

cludes 0.00 (no response to scattering); however, we note that none of the tests with pure white aerosol showed a response less than 0.01 times the scattering (see Figures 6 and 7).

Figure 6 shows the apparent absorption read by the three PSAPs when measuring a white aerosol. We performed an additional experiment to test the relationship between the ap-

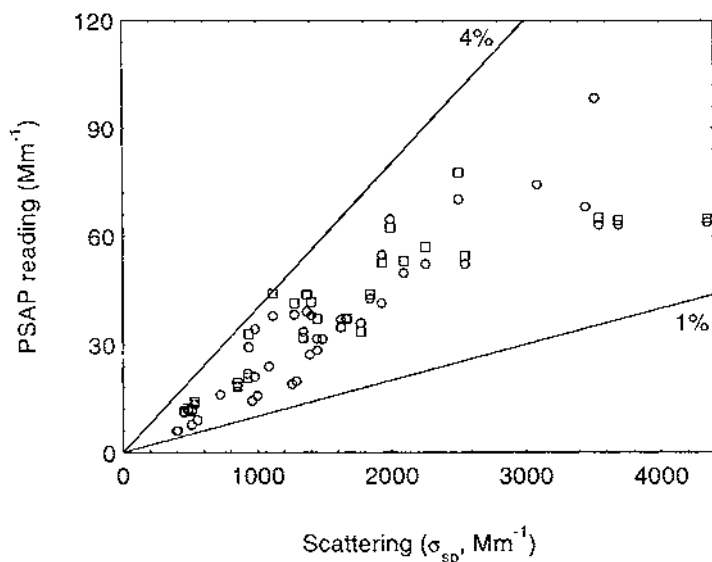


FIGURE 6. Apparent absorption: response of PSAP to nonabsorbing particles.

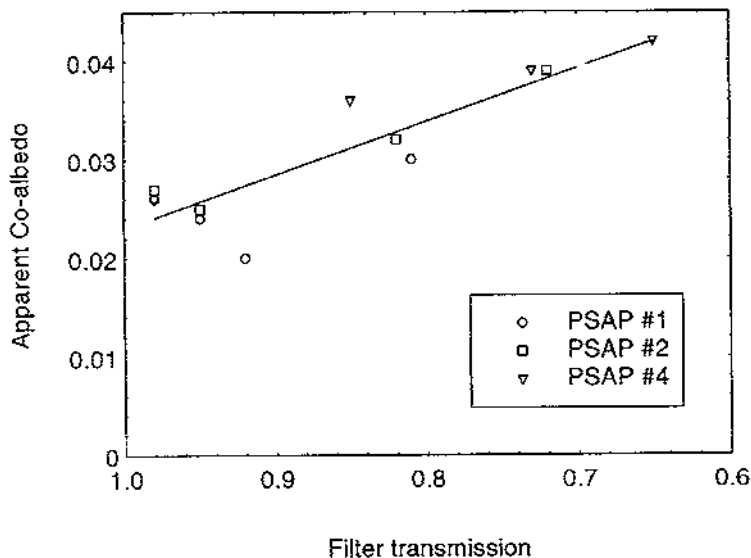


FIGURE 7. Artifact absorption of white aerosol when the filter has been previously loaded with absorbing aerosol. The filter transmission indicates the amount of previous loading (mainly with nigrosin).

parent absorption due to scattering aerosol and the amount of absorbing aerosol on the filter. We operated 3 PSAPs in parallel, loading each instrument with a different amount of absorbing aerosol before measuring the same white aerosol. The results are shown in Figure 7. The y axis shows the apparent coalbedo ($1 - \omega_0$) of the white aerosol; the filter transmission, which indicates the amount of nigrosin loading on the filter, is shown on the x axis.

The lowest transmission corresponds to the largest amount of dark particles on the filter; these conditions, where a pure white aerosol is sampled over highly absorbing particles, would rarely be encountered in practice. At the highest transmission, where there is no absorbing aerosol on the filter, the apparent absorption is 2% of the scattering. The latter is the response to scattering found in the calibration data when internally-mixed aerosols are used. Figure 7 suggests that the scattering response increases when scattering and absorbing aerosols are externally mixed *on the filter*.

The calibration experiments described here were performed with submicrometer aerosol. When an aerosol that included a coarse mode (up

to 5 μm aerodynamic diameter) was included, the value of K_1 decreased to 0.014, possibly because backscattering by coarse particles is lower than backscattering by fine particles. The fraction of the response attributable to submicrometer aerosol is not known, but the response to scattering aerosol appears to be much lower in the coarse mode than in the fine mode. For measurements of nonabsorbing, primarily coarse-mode aerosols (e.g., uncontaminated sea salt), the appropriate value might be as low as 0.01.

The instrument response to scattering aerosol can be obtained without measurements of reference absorption by measuring a nonabsorbing aerosol with both the PSAP and a nephelometer. Analysis of our tests in this manner gave nearly the same values as the least-squares analysis given in Table 4.

PSAP response to absorption

The PSAP reading, corrected for the scattering response, is shown in Figure 8. The derived value of K_2 is 1.22 ± 0.11 . The values presented in Figure 8 and used to calculate K_2 are the readings of the PSAP corrected for flow rate

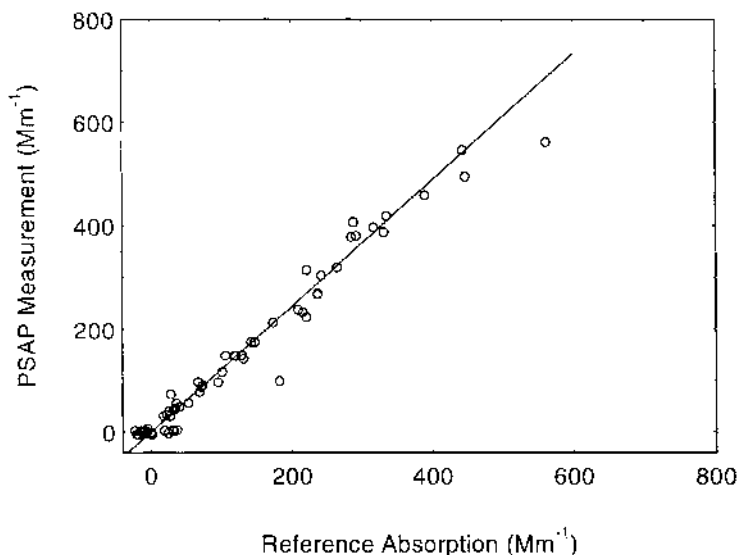


FIGURE 8. PSAP measurement (with 2% of measured scattering subtracted) versus reference absorption. The slope of the line is 1.22.

and spot size. Since the manufacturer's calibration has already been incorporated into the PSAP readings, our analysis suggests an *additional* 22% correction to that calibration.

We also suggest that the uncertainty in K_2 (0.11) should be increased to account for additional uncertainties, such as the difference between atmospheric and laboratory aerosols in terms of size, morphology, and composition. Although the present experiments cannot quantify these effects, we believe that the current uncertainty in K_2 is no smaller than 0.20.

PSAP Correction

The adjustment to and uncertainties in the PSAP are summarized below:

$$\sigma_{\text{ap}} = \frac{\sigma_{\text{adj}} - K_1 \sigma_{\text{sp}} + \epsilon_{\text{slope}} + \epsilon_{\text{noise}}}{K_2}, \quad (12)$$

where $K_1 = 0.02 \pm 0.02$, $K_2 = 1.22 \pm 0.20$, σ_{adj} is the reported value after the flow and spot size corrections, σ_{sp} is the scattering coefficient at 550 nm, and ϵ_{slope} and ϵ_{noise} are defined in Equations (7) and (8).

Intercomparison

The responses of the IP and the HIPS to scattering and absorbing aerosol, also determined using the statistical analyses described previously on the reference measurements of scattering and absorption, are given in Table 4. In practice, the uncertainty in K_2 for the IP should be increased because the collection efficiency of the Nuclepore filter depends on the size distribution.

All of the instruments exhibit *some* apparent absorption due to purely scattering aerosol. The largest response to scattering aerosol is for the integrating plate, for which 9% of the scattering appears as apparent absorption. This high value is to be expected, as this method does not embed particles within a filter nor is a change in backscattered light accounted for.

Each of the filter-based measurements has a K_2 greater than unity. That is, all the measure-

ments are higher than the reference absorption. The exaggeration of the absorption response is similar for the three methods; the measurements differ the most in their response to scattering.

The IP and HIPS readings are plotted against the PSAP readings in Figure 9, with different symbols used for each aerosol composition. The instrument readings have been adjusted by the factors shown in Table 4. If the linear model used to adjust each instrument were perfect, each point would lie within the error bounds of the 1:1 line. A large difference between two instruments suggests either measurement error or deviations from the linear model for one or both instruments.

For the IP (Figure 9a), the graph includes data for which no reference absorption is available (pure nigrosin and external mixtures). These points lie below the equality line; either the adjusted IP is too low or the adjusted PSAP reading is too high. The enhanced absorption response of the PSAP that was discussed previously may explain this difference for the external mixtures. The other points (those marked an76, an90, an95, and amsu) were those used to determine K_1 and K_2 and generally agree. However, a slight trend in the deviation with single-scatter albedo can be observed for the absorbing aerosols; those with $\omega_0 = 0.95$ (an95) lie slightly above the line, while those with $\omega_0 = 0.76$ (an76) lie slightly below it. In Figure 9b, the HIPS measurements show somewhat greater deviation from the line than do the IP measurements. The trend with single-scatter albedo just described for the IP is more pronounced for the HIPS.

The accurate measurement of absorption is important for the estimation of single-scatter albedo (ω_0). Figure 10 shows values of ω_0 , derived from the adjusted measurements of absorption and nephelometer measurements, plotted against the reference value of ω_0 , derived from extinction cell and nephelometer measurements. For the PSAP and the IP, 90% of the ω_0 are within 0.03 of the reference value. For ω_0 derived from the HIPS, 90% of the values are within 0.06 of the reference value.

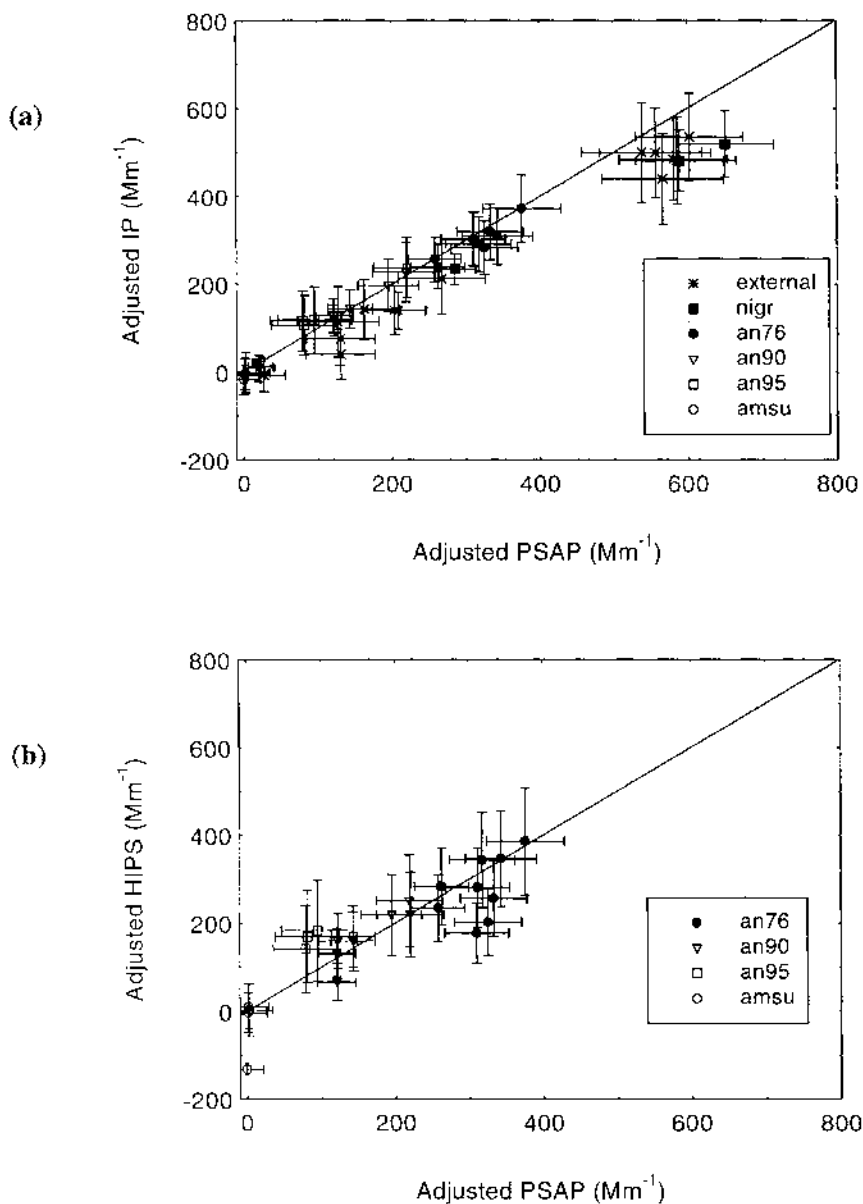


FIGURE 9. Intercomparison of instruments: (a) IP and PSAP and (b) HIPS and PSAP. All instruments have been adjusted according to the factors in Table 3. The error bars are 2- σ estimates. The legend refers to the aerosol composition given in Table 2.

SUMMARY

We have presented a calibration of the PSAP against an empirical method of measuring light absorption by particles suspended in the atmo-

sphere. The instrument is found to interpret about 2% of the scattering as absorption; after correcting for this effect, the measured absorption is about 22% higher than the reference

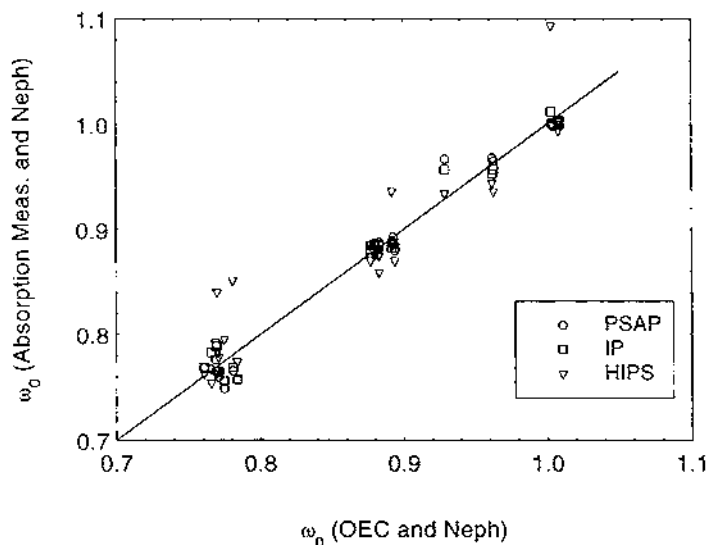


FIGURE 10. Inferred single-scatter albedo. The absorption measurements were adjusted by the factors shown in Table 4 prior to calculation.

absorption. We have also recommended corrections for differences in the flow measurement and spot size for individual PSAPs.

All filter-based measurements of absorption show some response to scattering by particles. The percentage of scattering that is measured as absorption is 4% for the HIPS and 9% for the IP. Even when the artifact due to scattering is removed, the absorption measured by the IP and the HIPS is too high by 23% and 32%, respectively.

Using any of the filter-based measurements without correction would result in single-scatter albedos that are too low, overestimating the effect of absorption on radiative transfer. The scheme we present here could be used to improve the accuracy of historical data sets. However, we caution that this calibration, which is based on a single absorbing species (nigrosin internally mixed with nonabsorbing ammonium sulfate), has not been demonstrated to apply to the full variety of atmospheric aerosols. Extending these results to realistic aerosols should have a high priority in future research in this area.

We gratefully acknowledge the support of the National Science Foundation under grant ATM-9320871, the National Oceanic and Atmospheric Administration under JISAO Agreement NA37RJ0198 (contribution number 586), and the Fannie and John Hertz Foundation. Dr. Kevin Perry participated in the operation of the IMPROVE samplers at the University of Washington. We thank Dr. Ray Weiss of Radiance Research, Dr. Dean Hegg of the University of Washington and Dr. Nels Laulainen of Battelle-Pacific Northwest Laboratories for loans of equipment. We thank Dr. Jost Heintzenberg and Dr. George Mulholland for their thorough comments.

References

- Adams, K. (1989). Real-Time in-situ Measurements of Atmospheric Optical Absorption in the Visible via Photoacoustic Spectroscopy. 1: Evaluation of Photoacoustic Cells, *Appl. Opt.* 27:4052–4056.
- Anderson, T. L., Covert, D. S., et al. (1996). Performance Characteristics of a High-Sensitivity, Three-Wavelength, Total Scatter/Backscatter Nephelometer, *J. Atm. Ocean. Tech.* 13:967–986.
- Anderson, T. L., Covert, D. S., et al. (1998). Aerosol Single Scatter Albedo: Values and Uncertainty at a Coastal Station in the Pacific Northwest, *J. Geophys. Res.*, submitted.

- Anderson, T. L., and Ogren, J. A. (1998). Determining Aerosol Radiative Properties using the TSI 3563 Integrating Nephelometer, *Aerosol Sci. Tech.* 29:57–69.
- Arnott, W. P., Moosmüller, H., Rogers, C. F., et al. (1999). Photoacoustic Spectrometer for Measuring Light Absorption by Aerosol: Instrument Description, *Atmos. Env.*, 33:2845–2852.
- Bennett, C. A. J., and Patty, R. R. (1982). Monitoring Particulate Carbon Collected on Teflon Filters: An Evaluation of Photoacoustic and Transmission Techniques, *Appl. Opt.* 21:371–374.
- Bergstrom, R. W. (1973). Extinction and Absorption Coefficients of the Atmospheric Aerosol as a Function of Particle Size, *Contr. Atm. Phys.* 46: 223–234.
- Bodhaine, B. A. (1995). Aerosol Absorption Measurements at Barrow, Mauna Loa and the South Pole, *J. Geophys. Res.* 100:8967–8975.
- Bodhaine, B. A., Harris, J. M., et al. (1992). Aerosol Optical Properties at Mauna Loa Observatory: Long-Range Transport from Kuwait? *Geophys. Res. Lett.* 19:581–584.
- Campbell, D., Copeland, S., and Cahill, T. (1995). Measurement of Aerosol Absorption Coefficient from Teflon Filters using Integrating Plate and Integrating Sphere Techniques, *Aer. Sci. Tech.* 22:287–292.
- Clarke, A. D. (1982a). Effects of Filter Internal Reflection Coefficient on Light Absorption Measurements Made using the Integrating Plate Method, *Appl. Opt.* 21:3021–3030.
- Clarke, A. D. (1982b). Integrating Sandwich: A New Method of Measurement of the Light Absorption Coefficient for Atmospheric Particles, *Appl. Opt.* 21:3011–3020.
- Clarke, A. D. (1989). Aerosol Light Absorption by Soot in Remote Environments, *Aer. Sci. Tech.* 10:161–171.
- Clarke, A. D., Noone, K. J., et al. (1987). Aerosol Light Absorption Measurement Techniques: Analysis and Intercomparisons, *Atmos. Env.* 21:1455–1465.
- Dobbins, R. A., Mulholland, G. W., and Bryner, N. P. (1994). Comparison of a Fractal Smoke Optics Model with Light Extinction Measurements, *Atmos. Env.* 28:889–897.
- Edwards, J. D., Ogren, J. A., et al. (1983). Particulate Air Pollutants: A Comparison of British "Smoke" with Optical Absorption Coefficient and Elemental Carbon Concentration, *Atmos. Env.* 17: 2337–2341.
- Fischer, K. (1970). Measurements of Absorption of Visible Radiation by Aerosol Particles. *Contr. Atmos. Phys.* 43:244–254.
- Garvey, D. M., and Pinnick, R. G. (1983). Response Characteristics of the Particle Measuring Systems Active Scattering Aerosol Spectrometer Probe (ASASP-X), *Aer. Sci. Tech.* 2:477–488.
- Gerber, H. E., and Hindmann, E. E. (1982). Light Absorption by Aerosol Particles, Spectrum Press, Hampton, VA.
- Hansen, A. D. A., Rosen, H., and Novakov, T. (1982). Real-Time Measurement of the Absorption Coefficient of Aerosol Particles, *Appl. Opt.* 21: 3060–3062.
- Heintzenberg, J. (1982). Size-Segregated Measurements of Particulate Elemental Carbon and Aerosol Light Absorption at Remote Arctic Locations, *Atmos. Env.* 16:2461–2469.
- Heintzenberg, J., Charlson, R. J., et al. (1997). Measurements and Modelling of Aerosol Single-Scattering Albedo: Progress, Problems and Prospects, *Contr. Atmos. Phys.* 70:249–263.
- Heintzenberg, J., and Leck, C. (1994). Seasonal Variation of the Atmospheric Aerosol Near the Top of the Marine Boundary Layer over Spitsbergen Related to the Arctic Sulphur Cycle, *Tellus* 46B: 52–67.
- Horvath, H. (1997). Experimental Calibration for Aerosol Light Absorption Measurements using the Integrating Plate Method—Summary of the Data, *Aerosol Sci.* 28:1149–1161.
- Justus, B. L., Huston, A. L., and Campillo, A. J. (1993). Broadband Thermal Optical Limiter, *Appl. Phys. Lett.* 63:1483–1485.
- Lin, C.-I., Baker, M., and Charlson, R. J. (1973). Absorption Coefficient of Atmospheric Aerosol: A Method for Measurement, *Appl. Opt.* 12: 1356–1363.
- Liu, B. H., and Lee, K. W. (1976). Efficiency of Membrane and Nuclepore Filters for Submicrometer Aerosols, *Env. Sci. Tech.* 10:345–350.
- Malm, W. C., Molenar, J. V., et al. (1996). Examining the Relationship Among Atmospheric Aerosols and Light Scattering and Extinction in the Grand Canyon Area, *J. Geophys. Res.* 101:19251–19265.
- Malm, W. C., Sisler, J. F., et al. (1994). Spatial and Seasonal Trends in Particle Concentration and Optical Extinction in the United States, *J. Geophys. Res.* 99:1347–1370.
- Moosmüller, H., Arnott, W. P., et al. (1998). Photoacoustic and Filter Measurements Related to Aerosol Light Absorption during the North-

- ern Front Range Air Quality Study (Colorado 1996/1997), *J. Geophys. Res.* 103:28, 149–28, 157.
- Petzold, A., Kopp, C., and Niessner, R. (1997). The Dependence of the Specific Attenuation Cross-Section on Black Carbon Mass Fraction and Particle Size, *Atmos. Env.* 31:661–672.
- Quinn, P. K., Coffman, D. J., et al. (1998). Aerosol Optics in the Marine Boundary Layer during ACE-1 and the Underlying Chemical and Physical Aerosol Properties, *Journal of Geophysical Research* 103:16547–16563.
- Ruoss, K., Dlugi, R., and Weigl, C. (1992). Intercomparison of Different Aethalometers with an Absorption Technique: Laboratory Calibrations and Field Measurements, *Atmos. Env.* 26A: 3161–3168.
- Sadler, M., Charlson, R. J., et al. (1981). An Intercomparison of the Integrating Plate and the Laser Transmission Methods for Determination of Aerosol Absorption Coefficients, *Atmos. Env.* 15:1265–1268.
- van de Hulst, H. C. (1957). *Light Scattering by Small Particles*, Dover Publications, Inc., New York, section 6.4.
- Waggoner, A. P., Weiss, R. E., et al. (1981). Optical Characteristics of Atmospheric Aerosols., *Atmos. Env.* 15:1891–1909.
- York, P. (1966). Least-Squares Fitting of a Straight Line, *Can. J. Phys.* 44:1079–1086.

Received August 21, 1998; accepted January 18, 1999.